Propagation of an ultrashort, intense laser pulse in a relativistic plasma

Burke Ritchie and Christopher D. Decker
Lawrence Livermore National Laboratory, University of California, Livermore, California 94550
(Received 6 June 1997; revised manuscript received 28 October 1997)

A Maxwell-relativistic fluid model is developed for the propagation of an ultrashort, intense laser pulse through an underdense plasma. The separability of plasma and optical frequencies (ω_p and ω, respectively) for small ω_p/ω is not assumed; thus the validity of multiple-scales theory (MST) can be tested. The theory is valid when ω_p/ω is of order unity or for cases in which $\omega_p/\omega \ll 1$ but strongly relativistic motion causes higher-order plasma harmonics to be generated which overlap the region of the first-order laser harmonic, such that MST would not be expected to be valid, although its principal validity criterion $\omega_p/\omega \ll 1$ holds. [S1063-651X(98)04304-9]

PACS number(s): 52.25.−b

I. INTRODUCTION

There is widespread interest in the propagation of subpicosecond, intense laser pulses through underdense plasmas in inertial confinement fusion [1], in wake-field acceleration [2], and in relativistic self-focusing and channel formation [3–5]. Theoretical approaches include particle-in-cell simulations (PIC) [6] and plasma fluid models [7–10].

On a time scale which is short compared to characteristic collision times, plasma electrons are accelerated by the laser to relativistic speeds, such that the electromagnetic fields and plasma are coupled nonlinearly through the Lorentz factor of special relativity,

$$\gamma = \left(1 + \frac{p^2}{m^2 c^2}\right)^{1/2}, \tag{1}$$

where $\vec{p}$ is the particle (or fluid) momentum. When one considers how the momentum is coupled to the fields in the equation of motion, then it is clear that the usual assumption that the fields can be represented by a single Fourier component at a ''carrier'' frequency cannot, in general, be made. Nevertheless if the plasma is sufficiently underdense, such that the plasma to optical frequency ratio ω_p/ω is small, where $\omega_p = \sqrt{4\pi e^2 n_e/m}$, and n_e is the electron density, then one can approximately eliminate the optical frequency to derive field and fluid slowly-varying-envelope (SVE) equations which vary on the scale of the plasma frequency. This approximation depends on a multiple-scales theory (MST) presented formally and implemented by Feit *et al.* [7] and by others previously [8–10] in problems of practical interest.

Approximations other than SVE are also made, for example, the quasistatic approximation (QSA) [8–10], whereby electrons are assumed to experience a static field on the scale of the laser pulse length. In other words, electrons can travel the length of the pulse before the pulse is altered significantly by diffraction, which is satisfied for pulse lengths much smaller than a Rayleigh range. The use of these approximations means that, unfortunately, current fluid models do not have the generality of the PIC model to facilitate mutual code comparison and benchmarking. Although PIC codes are generally valid over a wide range of regimes, it is desirable to have a more generally valid fluid code principally because PIC models tend to suffer from poor statistical resolution of the motion due to practical limitations in the number of particles which can be handled.

It is the purpose of this paper to present a relativistic fluid model in which neither the approximate separation of optical and plasma time scales of MST nor the QSA dynamical approximation is made. The fluid model results are then benchmarked against PIC results as a test of our numerical methods.

II. THEORY AND NUMERICAL METHODS

The equations of the model are Maxwell's equations for the vector and scalar potentials in the Lorentz gauge, the continuity equation, and the fluid momentum equations:

$$\left(\nabla^2 - \frac{1}{c^2}\frac{\partial^2}{\partial t^2}\right)\vec{A} = -\frac{\omega_p^2 n \vec{p}}{e\gamma c}, \tag{1a}$$

$$\left(\nabla^2 - \frac{1}{c^2}\frac{\partial^2}{\partial t^2}\right)\Phi = -\frac{m\omega_p^2 (n - n_i)}{e}, \tag{1b}$$

$$\frac{\partial n}{\partial t} = -\vec{\nabla}\cdot\left(\frac{\vec{p} n}{m\gamma}\right), \tag{1c}$$

$$\left(\frac{\partial}{\partial t} + \frac{\vec{p}\cdot\vec{\nabla}}{m\gamma}\right)\cdot\vec{p} = -\frac{e}{c}\frac{\partial \vec{A}}{\partial t} - \vec{\nabla} e\Phi + \frac{e}{mc\gamma}(\vec{p}\times\vec{\nabla}\times\vec{A}). \tag{1d}$$

In Eqs. (1), n is the dimensionless normalized electron density and n_i the dimensionless normalized ion density, which is taken to be constant during the passage of a laser with a pulse length in the femtosecond regime.

We differentiate Eqs. (1a) and (1b) in time but not in space, where the spatial problem is defined as a two-dimensional slab with propagation along z. The use of fast Fourier transform (FFT) methods to treat spatial derivatives has been described previously [11]; here we merely outline the techniques used for the equations of the Maxwell-fluid model. All terms containing differential operators are moved to the right side, which is assumed known from the previous time step. Then we Fourier transform the equations in space and advance the resulting algebraic equations one time step using the three-point central-difference algorithm for the

second-order time derivative. Then we find the inverse Fourier transform. This constitutes one cycle in the temporal advance. We treat Eq. (1d) similarly, a procedure which has already been implemented by others [12] for the fluid momentum.

In this way, spatial differencing is entirely avoided. This procedure has the effect that spatial derivatives, which in real-space, finite-difference methods are distributed locally over a selected number of grid zones, and can be the source of numerical instabilities, are smoothed globally over all space, thereby leading to robustly stable results. We use the standard FFT routine of Cooley and Tukey [13], which is a very fast algorithm on a vector machine. This procedure, as applied to Maxwell's equations, was thoroughly benchmarked in other applications [11].

A similar procedure, applied to Eq. (1c), however, does not yield numerically stable results. The following procedures, however, do yield numerically stable results. Our algorithm to advance the normalized electron density over an interval dt is

$$n_a = e^{-(dt/2m\gamma)\vec{p}\cdot\vec{\nabla}} e^{-dt\vec{\nabla}\cdot\vec{p}/m\gamma} e^{-(dt/2m\gamma)\vec{p}\cdot\vec{\nabla}} n_r, \qquad (2)$$

where the subscripts a and r designate the advanced, retarded function with respect to the interval dt. This algorithm is a form of the well-known split-operator FFT method [14], in which noncommuting exponential factors of the propagator are arranged over a single three-step interval, as shown in Eq. (2). The outside factors, which contain differential operators, are evaluated in transform space, and the middle factor is evaluated in real space. This procedure is obviously limited to first-order accuracy in dt because (in contrast to the conventional split-operator method of Ref. [14]) $\vec{p}/\gamma$ depends on space, and thus higher-order noncommuting terms in the expansion of the exponential are dropped as truncation errors. However, this procedure is observed to be conditionally numerically stable, as determined by the Courant condition $c\Delta t/\Delta s < 1$ (where s is a spatial coordinate), as expected for an explicit advance in a convection equation.

III. RESULTS AND DISCUSSION

The laser wavelength is 1 μm. The plasma density is 10^{20} cm^{-3}, such that the ratio of the plasma to optical frequency, ω_p/ω, is 0.296. In the calculations we use the scaled variables: time in units of ω^{-1}, space in units of k^{-1}, fields in units of mc^2/e, and momentum in units of mc. The longitudinal and transverse widths of the Gaussian pulse are 10 and 17.67 k^{-1}, respectively, where the full width at half maximum is $2\delta\sqrt{\ln 2}$ for a Gaussian width δ. This corresponds to a pulse length of about 8.75 fs and a pulse width of about 4.64 μm. For a maximum time of $220\omega^{-1}$, a transverse length of 125 k^{-1}, and longitudinal length of 500 k^{-1}, we used 8001, 256, and 1024 mesh points, respectively.

The PIC calculations were performed using the code WAVE [15], which has been thoroughly benchmarked over the last two decades [16]. We used 10^6 particles (sufficient to resolve the fifth-order laser harmonic) and 512 and 256 mesh points for longitudinal and transverse lengths, respectively, equal to 204.8 k^{-1}. The temporal interval is $0.2\omega^{-1}$.

Aside from inherent differences between the fluid and PIC models, the linear polarization of the laser lies in the plane of the plasma for the fluid code, and lies perpendicular to the plane of the plasma for the PIC code, a difference which unfortunately seemed to require more code labor to rectify than was available. However, from the comparison of the results it appears that the polarization difference shows up primarily in the spectra of the wake electromagnetic (EM) field, which for the PIC model is absent a peak at the laser frequency, as expected on theoretical grounds.

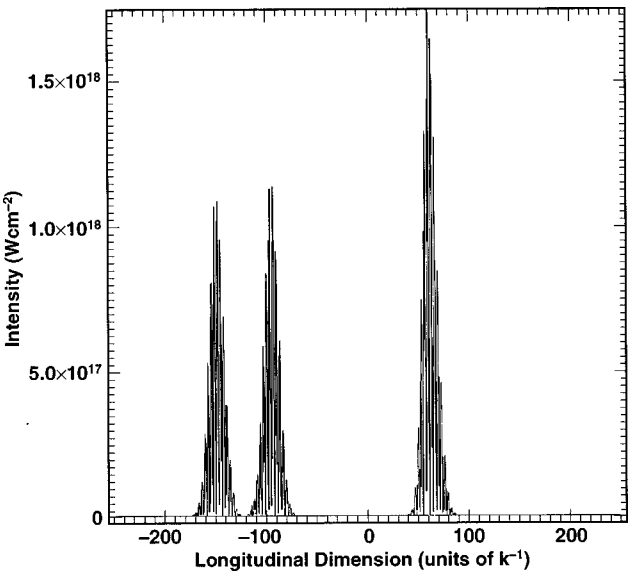

FIG. 1. Three snapshots of laser intensity vs longitudinal distance. The laser enters the region of the plasma at $-100\,k^{-1}$, and is self-focused as it passes through the region.

We present results for a laser pulse with a peak intensity of 1.12×10^{18} W cm^{-2} (Fig. 1) incident on a cold plasma whose boundaries are sharply defined at -100 and $100\,k^{-1}$ longitudinally and at the grid boundaries transversely. The laser is polarized in the transverse direction, and causes the transverse component of the fluid momentum to quiver as shown in Fig. 2. The EM fields are calculated from the po-

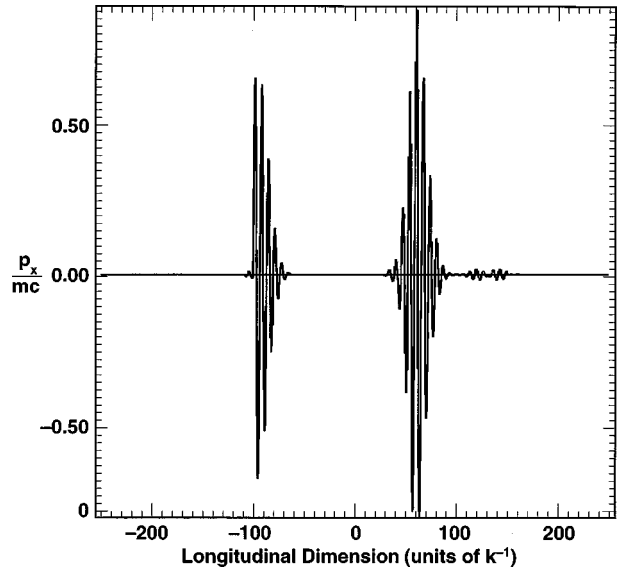

FIG. 2. Snapshots of fluid quiver momentum vs longitudinal distance corresponding to the second and third snapshots from the left of Fig. 1. The periodicity is on the optical frequency scale.

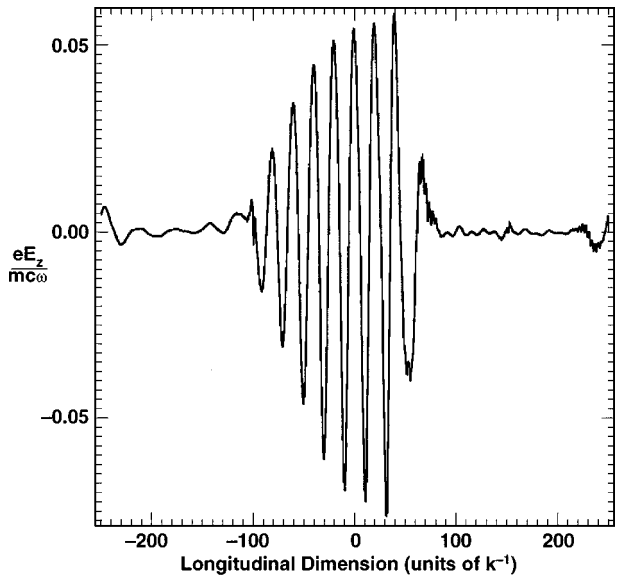

FIG. 3. Wake EM field vs longitudinal distance for the right-hand pulse of Fig. 1. The periodicity is on the plasma frequency scale, with optical-scale modulation clearly visible near the form of the pulse.

tentials [Eqs. 1(a) and 1(b)] from the relation

$$\vec{E} = -\frac{1}{c}\frac{\partial \vec{A}}{\partial t} - \vec{\nabla}\Phi. \tag{3}$$

In the wake of the laser, a longitudinal EM field is generated (Figs. 3 and 4) which extends for many plasma wavelengths—a plasma wavelength is $2\pi\,\omega/\omega_p$ in our scaled variables. The fluid and PIC models in Figs. 3 and 4, respectively, show reasonable mutual agreement considering their theoretical differences. The poorest agreement is observed near the laser pulse and at the left-hand boundary of the

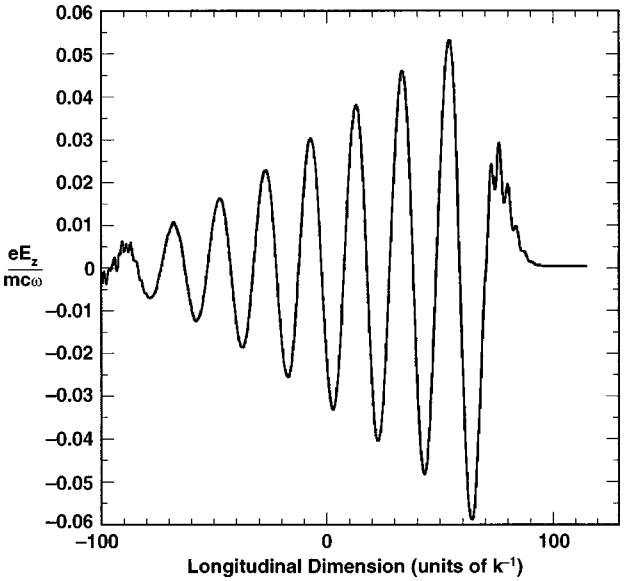

FIG. 4. Wake EM field as given by the PIC model vs longitudinal distance as a comparison with the fluid-model wake field given in Fig. 3.

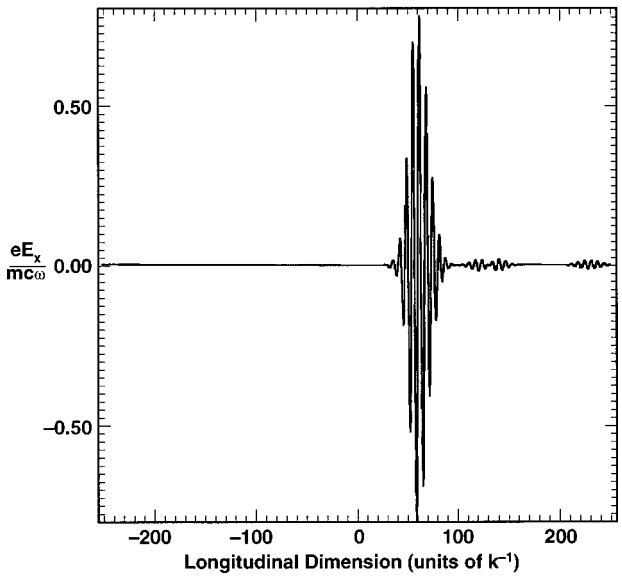

FIG. 5. Laser EM field vs longitudinal distance for the right-hand pulse of Fig. 1 for purposes of comparison of magnitude and shape with the wake field of Fig. 3.

plasma. This may reflect the use of damping terms in the fluid momentum equations to suppress motion outside of the plasma boundaries.

The authors of Ref. [7] neglected the wake vector potential [Eq. 1(a)], which is polarized along the direction of propagation of the pulse, on the grounds that their calculation is in a weakly relativistic regime (their rms laser intensity is 1.1×10^{17} W cm^{-2}, for which the electron quiver momentum is about $0.28mc$). On the other hand, our calculations at a rms intensity of 5.6×10^{17} W cm^{-2} (Fig. 1, right-hand pulse), for which the quiver momentum is about $0.9mc$ (Fig. 2, right-hand momentum), show that the electromagnetic wake field (Fig. 3) for an electron density n_e of 10^{20} cm^{-3} has a peak field strength which is about 10% of our laser peak field strength (Fig. 5), or about 2.4×10^{9} V/cm. The scaling law given by Eq. (2) in Ref. [9],

$$E_z/E_x \cong 1.2\times10^{-11}\sqrt{n_e[\mathrm{cm}^{-3}]}\lambda[\mu\mathrm{m}]a_0/\sqrt{(1+a_0^2/2)}, \tag{4}$$

where a_0 is the scaled quiver momentum (Fig. 2), states that the ratio of wake to laser peak field strengths should be about 9% for our parameter set; thus our observed ratio is in reasonable agreement. Although their ratio of wake to laser peak field strengths is only about 6% of our ratio, because their quiver velocity and electron density (about 2×10^{18} cm^{-3}) are smaller; nevertheless their wake peak field strength, according to Eq. (4), should be about 0.5% of their laser peak field strength or about 4.6×10^{7} V/cm. Although much much smaller than ours, this field is still clearly of non-negligible physical importance.

The wake field oscillates near the plasma frequency ω_p; however, due to the nonlinear nature of the forces driving the plasma, we observe harmonic generation to order $3\omega_p$ in the power spectrum of the wake field (Fig. 6). The spectrum is defined as the squared modulus of the temporal Fourier transform of the field at a single longitudinal point (here at $z=30\,k^{-1}$), integrated over the transverse direction. The

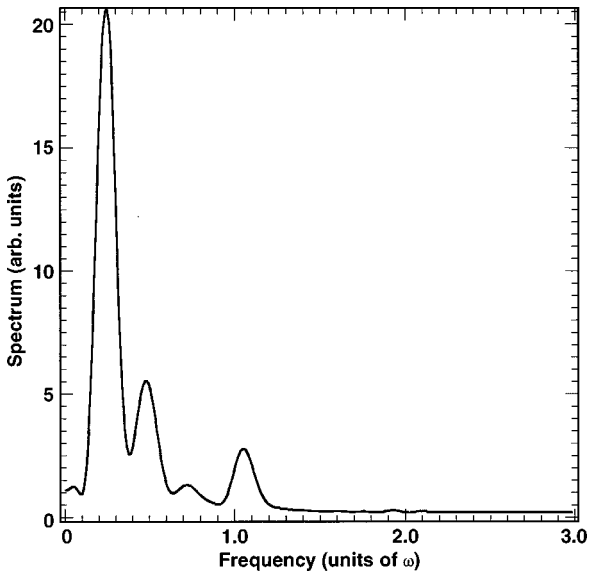

FIG. 6. Wake-field power spectrum, in units of the optical frequency (i.e., the fundamental optical frequency is one unit). Clearly visible are the first three redshifted plasma harmonics. The blue-shifted harmonic at the optical frequency arises because the polarization of the laser in the plane of the plasma induces motion in the electron density at the optical frequency. Less pronounced are the structures near zero, and two which are caused by the Lorentz-force contribution to the motion.

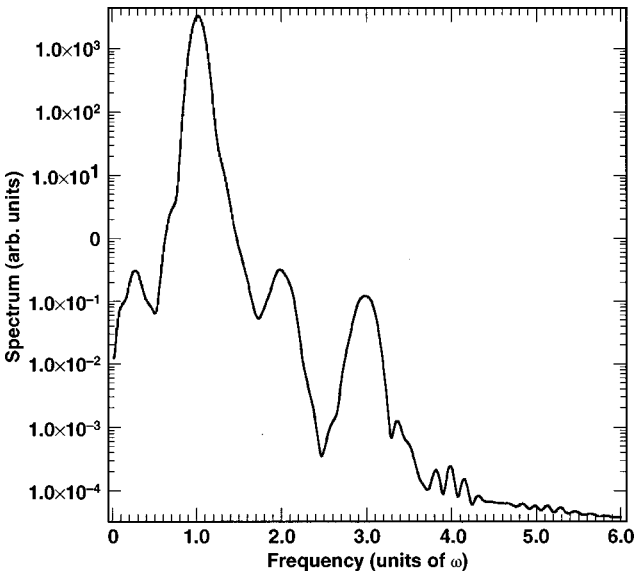

FIG. 7. Laser-field power spectrum, in units of the optical frequency (i.e., the fundamental optical frequency is one unit). The first, second, and third harmonics are well resolved, while the fourth and fifth harmonics are much less well resolved.

spectral peaks are redshifted slightly from the expected multiples of $\omega_p/\omega=0.296$ due to partial expulsion of plasma electrons from the laser's path (''ponderomotive expulsion''). Generation of harmonics in the pulse at the laser frequency [17] is also observed (Fig. 7).

IV. CONCLUSIONS

These comparative studies have taught us important lessons with respect to the validity and usefulness of previously published relativistic fluid codes. First, the third harmonic in the plasma harmonic series (Fig. 6) is very near the optical frequency ω (for our $\omega_p/\omega\sim 0.3$); thus one may be led to question the usefulness of the multiple-scales scheme to eliminate the optical frequency except in weakly relativistic regimes, as in Ref. [7], because clearly the approximate separation of frequencies in MST, although reasonably well supported by its principal validity criterion $\omega_p/\omega\ll 1$, would nevertheless not be expected to hold when higher-order members of the plasma harmonic series overlap strongly with the first-order optical harmonic, which could reasonably be expected to occur at higher laser intensities and a more strongly relativistic motion. Thus the plasma harmonic spectrum gives a more stringent test of the validity of MST than the inequality alone.

Second, it is not sensible to neglect the electromagnetic wake vector potential, as in Ref. [7], even in the weakly relativistic regime considered there. Although the accuracy of the results which these authors do present is likely not seriously impaired by this neglect, nevertheless their wake field has a peak field strength of about 4.6×10^7 V/cm [as we estimated from Eq. (4)], and clearly is important in giving an overall qualitatively accurate physical picture of intense laser propagation through a relativistic plasma.

Furthermore the condition $\vec{\nabla} n_e\times(\vec{\pi}-\vec{a})=0$, which holds if the electron density is spatially homogeneous and $\vec{\pi}$ and $\vec{a}$ are the momentum field and wake vector potential, respectively, which vary on the plasma time scale, is used by the authors of Ref. [7] to claim that the wake vector potential vanishes. Obviously this condition states only that $\vec{\nabla}\times\vec{\pi}=\vec{\nabla}\times\vec{a}$, and does not imply that the wake vector potential itself vanishes.

Finally a parallel version of the FFT algorithm is currently available, and has been implemented [18] by one of the authors of Ref. [11] in ion-atom charge exchange. This availability would be expected to enhance the attractiveness of FFT methods [11] for use in Maxwell-fluid and other multidimensional models.

ACKNOWLEDGMENTS

One of the authors (B.R.) wishes to thank Britton Chang, Machael Feit, John Garrison, and Merle Riley for helpful discussions. This work was performed under the auspices of the U.S. Department of Energy by the Lawrence Livermore National Laboratory under Contract No. W-7405-ENG-48.

[1] M. Tabak *et al.*, Phys. Plasmas **1**, 1626 (1994).

[2] J. Wurtele, in *Advanced Accelerator Concepts*, Proceedings of the Sixth Advanced Accelerator Concepts Workshop, Fontam, WI, June, 1994, edited by J. Wurtele, AIP Conf. Proc. No. 279 (AIP, New York, 1993).

[3] Guo-Zheng Sun, E. Ott, Y. C. Lee, and P. Guzdar, Phys. Fluids **30**, 526 (1987).

[4] A. B. Borisov, A. V. Borovskiy, O. B. Shiryaev, V. V. Korobkin, A. M. Prokhorov, J. C. Solem, T. S. Luk, K. Boyer, and C. K. Rhodes, Phys. Rev. A **45**, 5830 (1992); A. B.

Borisov, A. V. Borovskiy, V. V. Korobkin, A. M. Prokhorov, O. B. Shiryaev, X. M. Shi, T. S. Luk, A. M. McPherson, J. C. Solem, K. Boyer, and C. K. Rhodes, Phys. Rev. Lett. **68**, 2309 (1992).

[5] Burke Ritchie, Phys. Rev. E **50**, R687 (1994); P. R. Bolton and B. Ritchie, J. Opt. Soc. Am. B **14**, 437 (1997).

[6] C. D. Decker, W. B. Mori, and T. Katsouleas, Phys. Rev. E **50**, R3338 (1994).

[7] M. D. Feit, J. C. Garrison, and A. M. Rubenchik, Phys. Rev. E **53**, 1068 (1996).

[8] P. Sprangle, E. Esarey, J. Krall, and G. Joyce, Phys. Rev. Lett. **69**, 2200 (1992).

[9] E. Esarey, P. Sprangle, J. Krall, and G. Joyce, Phys. Fluids B **5**, 2690 (1993).

[10] J. Krall, A. Ting, E. Esarey, and P. Sprangle, Phys. Rev. E **48**, 2157 (1993); the simulation code used in Refs. [8–10] is described in the Appendix of J. Krall, E. Esarey, P. Sprangle, and G. Joyce, Phys. Plasmas **1**, 1738 (1994).

[11] B. Ritchie and M. E. Riley, Sandia Report No. Sand97-1205, UC-401, 1997 (unpublished); B. Ritchie, P. Dykema, and D. Braddy, Phys. Rev. E **56**, 2217 (1997).

[12] Vadim Borue and Steven A. Orszag, Phys. Rev. E **51**, R856 (1995).

[13] J. W. Cooley and J. W. Tukey, Math. Comput. **19**, 297 (1965).

[14] J. A. Fleck, Jr., J. R. Morris, and M. D. Feit, Appl. Phys. **10**, 129 (1976); M. D. Feit and J. A. Fleck, Jr., Appl. Opt. **17**, 3990 (1978).

[15] R. L. Morse and C. W. Nielson, Phys. Fluids **14**, 830 (1971).

[16] D. W. Forslund, J. M. Kindel, and E. Lindman, Phys. Fluids **8**, 1017 (1975); D. W. Forslund, J. M. Kindel, W. Mori, C. Joshi, and J. M. Dawson, Phys. Rev. Lett. **54**, 558 (1985); C. W. Decker, W. B. Mori, K.-C. Tzeng, and T. Katsouleas, Phys. Plasmas **3**, 2047 (1996).

[17] P. Sprangle, E. Esarey, and A. Ting, Phys. Rev. A **41**, 4463 (1990).

[18] M. E. Riley (private communication).